

Chapter 5:

Microhardness of $\text{InBi}_{1-x}\text{Te}_x$

Crystals

In this chapter, the results of microhardness of $\text{InBi}_{1-x}\text{Te}_x$ ($x=0.05, 0.10$ and 0.15 .) crystals are described. Microhardness indentation tests were carried out on the cleavage planes (001) of the $\text{InBi}_{1-x}\text{Te}_x$ ($x=0, 0.05, 0.10$ and 0.15) crystals using the Vickers diamond pyramidal indenter. It has also been studied how hardness varies with applied load in detail.

5.1 Introduction:

The most common method for determining the hardness of crystals, whether metallic or nonmetallic, is the indentation method. This approach does not require big specimens and multiple measurements can be performed on a tiny specimen. Friction and preceding strain hardening are two of the many elements that influence the measured value of hardness. The geometry of the indenter is also one of them. According to their incorporated angles of less or higher than 90° , the indenter employed corresponds to be either sharp or blunt. The indenter tends to be blunt as the angle increases. In the relationship between hardness (H) and yield stress (Y), namely, $H = CY$, the value of the constraint factor “C” is also important. It tends to 3 as the effective cone angle increases [1]. The stress field generated by such an indenter closely resembles the elastic theory prediction. The included angle of 136° on the Vickers diamond pyramidal indenter utilized in this work is a fair balance between minimizing frictional effects and producing a clearly defined geometrically formed indentation mark. The geometry of the indenter is shown below:

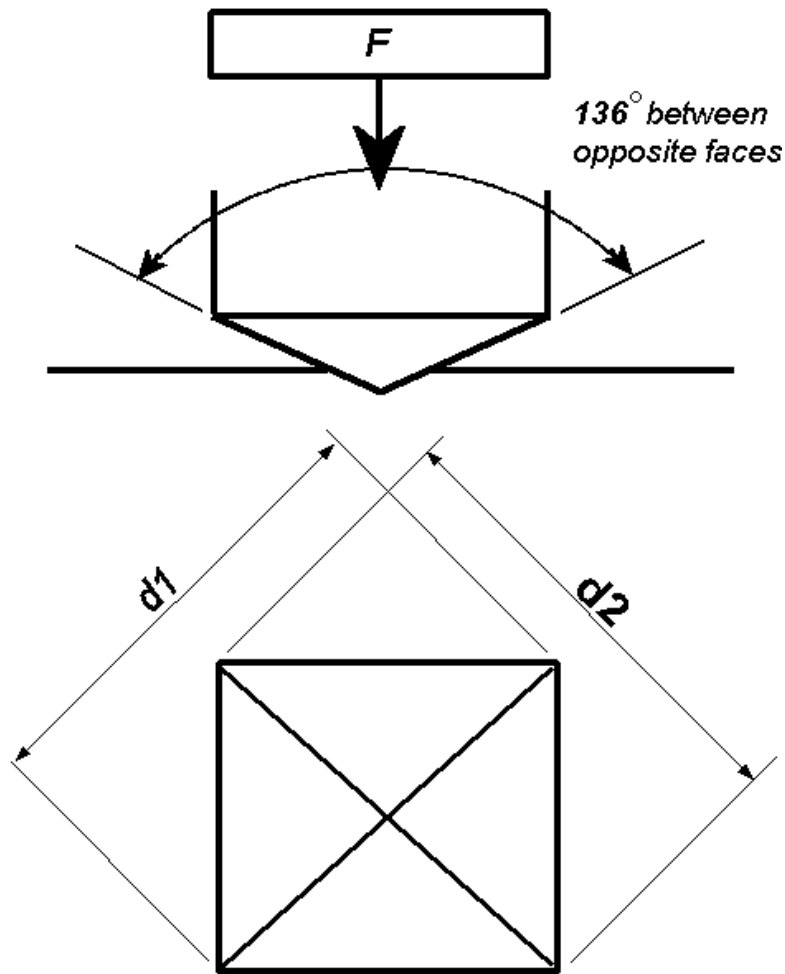


Figure 5.1: Vickers Indentor

The coefficient of friction between the diamond and the cleavage surface of a metal ranges between 0.1 and 0.15, making frictional effects less noticeable (Tabor) [2]. The Vickers hardness is defined as the ratio of applied load to the pyramidal contact area of indentation and it is calculated as

$$H_v = \frac{1854 \times p \times 9.80}{d^2} \text{ -----(5.1)}$$

where, H_v = Vickers microhardness in MPa, P = applied load in mN, d = mean diagonal length of the indentation mark in μm .

The indentation mark is geometrically reliable despite the size. This would entail that the hardness is independent of load. However, this is not the case and except for loads

exceeding around 200 gm (i.e., 1960 mN), the obtained hardness value has been found apparently to be load dependent in all the cases and thus hardness value calculated in the low load region (200gm, i.e., 1960 mN) is known as microhardness. Although, the cutoff load is not well defined and the hardness may accomplish a constant value for loads increasing in the range from 20 to 50 gm (i.e., 196 to 490 mN) or beyond, depending on the material and its mechanical history. Hardness varies with load in a complex fashion and does not follow any uniform norm in general. Many researchers have researched hardness, but the conclusions are somewhat perplexing. Bergsman [3] found that load had a considerable effect on hardness. Rostoker discovered a decrease in hardness when testing copper at modest applied stresses [4]. As the applied load is reduced, the diagonal length reduces and the hardness value increases.

Buckle discovered that hardness increased significantly at low applied stresses. Knoop et al. and Bernhardt discovered that the hardness increased with decreasing load [5, 6]. In contrast, Campbell et al. and Mott et al. observed a decrease in hardness with decreasing load. [7]. No apparent change in hardness with load variation was observed by Taylor [8] and Toman et al. [12]. Such contradictory results could be explained by the influence of the surface layers and vibrations generated during the indentation process. [5-13].

Gane et al investigated microhardness at extremely small loads and discovered an increase in hardness at small indentation sizes, hypothesizing that this could be due to the high stresses required for homogeneous dislocation nucleation in small dislocation-free indented regions. [14]. Ivan'ko, on the other hand, discovered a reduction in microhardness with decreasing load, concluding that this relationship is related to the influences of plastic and elastic deformations in the indentation process [15]. Based on these interpretation and reports, it is possible to conclude that microhardness and applied load do not necessarily have a relationship. As shown in equation 5.2, the hardness, to be independent of load P, should be directly proportional to the square of the diagonal length “d”. Thus,

$$P = ad^2 \text{ ----- (5.2)}$$

where “a” is a material constant. This expression is known as Kick’s law. According to the preceding discussion, the observed hardness dependence on load implies that the power index in this formula should be more than 2 and Hanemann [16] suggests that the general form of load dependence on diagonal length should be

$$P = ad^n \text{ ----- (5.3)}$$

The deviation in the value of the index ‘n’ from 2 indicates that the hardness changes with the load. As a result, this formula can be used to determine hardness variations with load.

The exponent 'n' in the formula is also known as Meyer index or logarithmic index. According to Hanemann [16] n is generally less than 2 for low load conditions, thus explaining the higher hardness at low loads. On the other hand, Mil'vidskii et al observed that "n" was between 1.3 and 4.9. [17].

It is inevitable that hardness would vary with load in the low load range. Increases in hardness have been reported in such a range. For high loads, the hardness is also found to reach a constant value regardless of the load used. In the case of polished and natural faces of NaCl single crystals, Boyarskaya attributed the rise in hardness with load to the penetrated surface layers and the dislocation content [18]. Yoshino discovered that the microhardness of aluminium and magnesium single crystals grew rapidly initially with increasing load, then progressively reduced and finally became independent of load [19]. The decrease in hardness with load is due to heterogeneous deformation and anisotropy.

Cleavage surfaces of the crystals were used for all indentation tests. Each indent was made on a freshly cleaved surface. The azimuthal orientation of the indenter with respect to the crystal surface must be maintained constant in order to avoid anisotropic variations in the measured hardness and it was done so. The diagonal of the indentation mark was oriented parallel to this direction using the initial indentation. Three indentations were made for each measurement and the average diagonal length was used to calculate hardness.

5.2 Vickers Microhardness of $\text{InBi}_{1-x}\text{Te}_x$ Crystals:

The indentations were done at specially slow pace and much care was taken to ensure that the pace was almost the same for each indentation. To avoid interference, a space of at least three indentations was maintained between two adjoining indentation marks on the same surface. It was a square shape indentation mark produced. The diagonals of the indentation mark were measured using a micrometer eyepiece with a least count of 0.19 micron. As previously indicated, indentations were made with a Vickers pyramidal diamond indenter at various loads ranging from 1 gm to 100 gm with fixed azimuthal orientations of the indenter to reduce anisotropic effects. The duration of the indentation was fixed at 30 seconds. Figures 5.2(a), (b), (c), (d) show plots of Vickers hardness H_v vs load P for $\text{InBi}_{1-x}\text{Te}_x$ ($x=0, 0.05, 0.1, \text{ and } 0.15$). The figures clearly show that hardness varies with load in a characteristic way. Starting with the smallest load and gradually increasing up to an applied load of about 50 gms, the hardness gradually increases. It reaches saturation at 50 gm. It is in good agreement with the reported microhardness value [20].

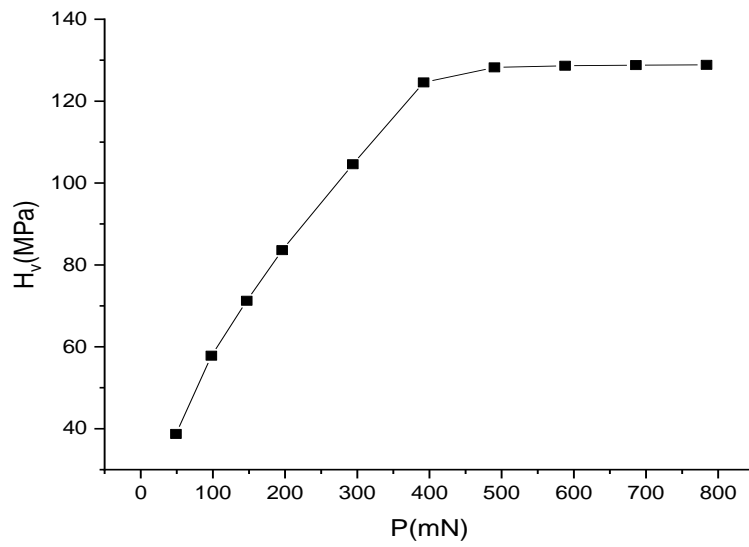


Figure 5.2(a): Plot of H_v versus P of InBi crystals

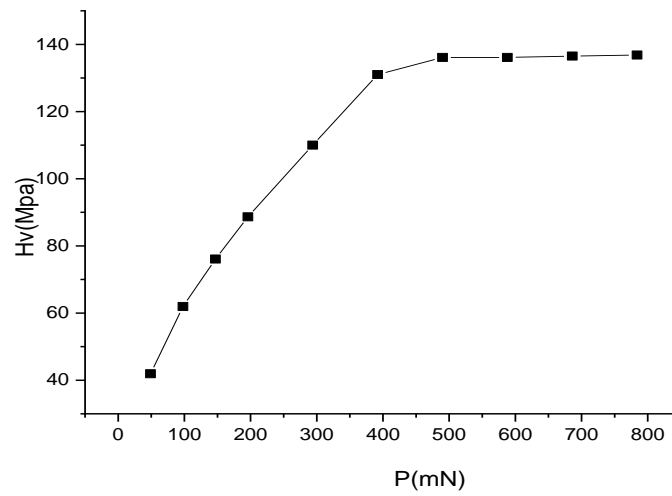


Figure 5.2(b): Plot of H_v versus P of $\text{InBi}_{0.95}\text{Te}_{0.05}$ crystals

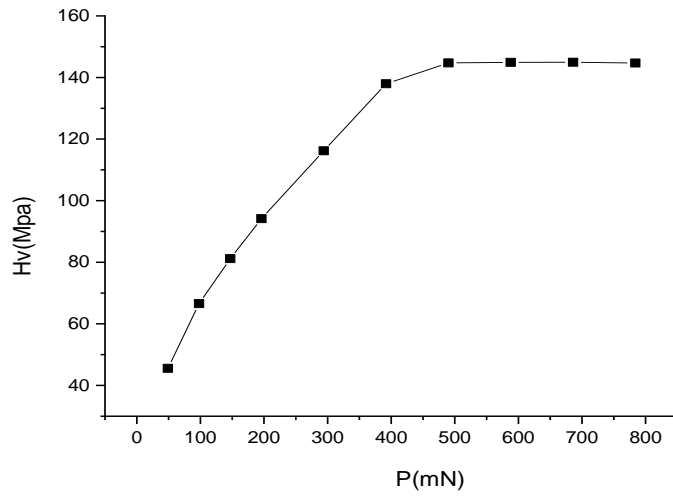


Figure 5.2(c): Plot of H_v versus P of $\text{InBi}_{0.80}\text{Te}_{0.10}$ crystals

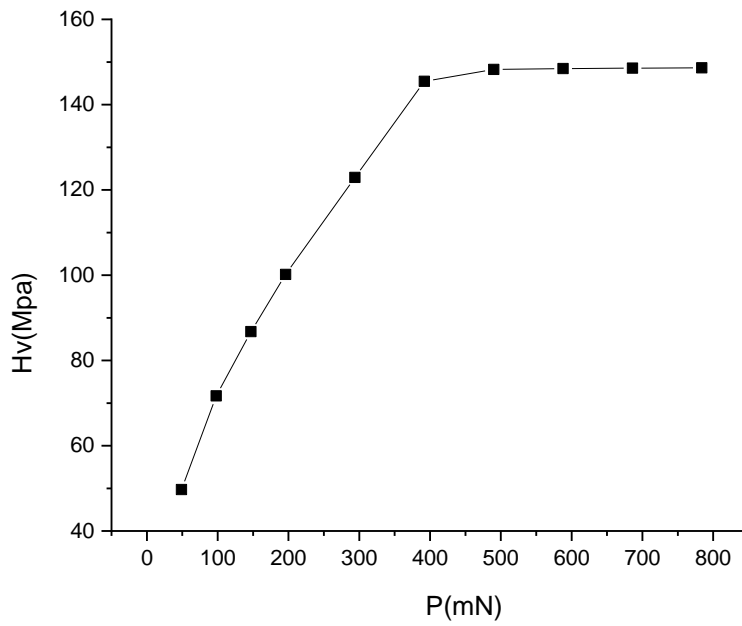


Figure 5.2(d): Plot of H_v versus P of $\text{InBi}_{0.85}\text{Te}_{0.15}$ crystals

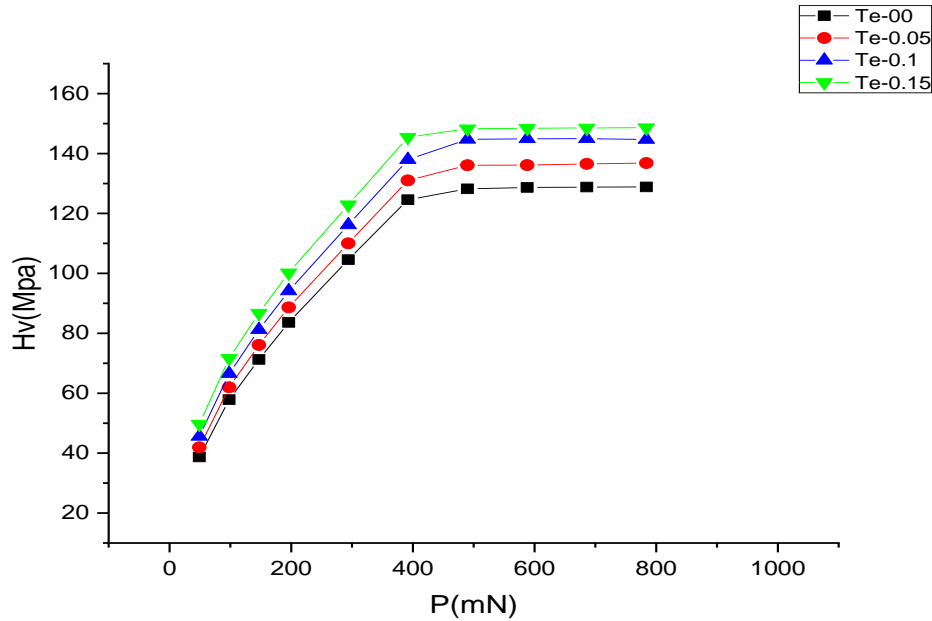


Figure 5.2(e): Plots of H_V versus P of $\text{InBi}_{1-x}\text{Te}_x$ ($x= 0, 0.05, 0.1, 0.15$) crystals

The work hardening ability and elastic resurgence of certain materials are dependent on the load, the type of surface getting the stress and the depth to which the surface is punctured by the indenter; thus, hardness varies dramatically in the low load area. The elastic recovery and piling up of material surrounding the indentation mark have been used to explain the low load hardness behavior of, for example, silicon single crystals [21]. Because the penetration depth is often greater than the work hardened surface layer at high loads, the microhardness at high loads will be reflective of the bulk and hence load independent. Even for surfaces where mechanical preparation is not required, for example, the hardness acquired at low stresses may differ from the hardness obtained at high loads on cleavage planes of metals and minerals.

Now the depth of penetration depends usually on three factors:

- 1) The kind of surface receiving the load. It can be separated into three categories:
 - surface layers with various degrees of cold working (Onitsch) [22].
 - surface layers with finely precipitated particles (Buckle) [23].
 - surface layers with various grain sizes (Bochvar et al) [24] and number of grains indented (Onitsch) [25].

- 2) The magnitude of the applied load
- 3) The accuracy for the normal indenting of the specimen and the rate at which it is done, i.e., the strain rate. The strain rate will obviously be determined by the time it takes to realize the full applied load.

All of these issues come into play when indentation testing is performed at low loads. The depth of penetration of the indenter can explain the fluctuation in hardness with load in the plot of H_v v/s P. Because the indenter can only penetrate surface layers at low loads, the effect is more obvious there. The effect of the crystalline surface layers becomes less evident as the depth of penetration increases, which helps to reduce the variation of microhardness when loads are higher. Once the inner layers of the sample have been penetrated to a certain depth, they progressively achieve supremacy over the outer layers and the hardness value no longer varies with load.

The results of microhardness variation with applied load are shown in Figure 5.2 (a - e), the H_v versus P plots, obtained for the as cleaved samples of $\text{InBi}_{1-x}\text{Te}_x$ ($x=0, 0.05, 0.1$ and 0.15) crystals. The hardness peaks can be explained in terms of the deformation-induced coherent zones that arise in surface regions under the indentation. The indenter penetrates the virgin surface layers and beyond a specific depth of penetration, which corresponds to the coherent zone span, the load reaches peak hardness [26-28, 32-33]. Beyond 490mN, the hardness is seen to be load independent and represents true or bulk hardness of the crystal. As a result, the microhardness values of $\text{InBi}_{1-x}\text{Te}_x$ ($x= 0, 0.05, 0.1$ and 0.15) crystals are 128 (in good agreement with reported hardness value [28]), 136, 144 and 148 MPa, respectively [Figures 5.2 (a - e)]. These are significantly higher than what is expected for a pure InBi crystal. As a result, all three dopant concentrations exhibit considerable impurity hardening.

5.3 Meyer's Index:

The Meyer's law is also valuable in analyzing reliance of microhardness on load. The law is

$$P = ad^n \text{----(5.4)}$$

where the index n is known as Meyer index and P =applied load and d= diagonal length of the indentation mark, Whereas, a= material constant. Load dependence of microhardness is reflected in the deviation of the value of n from 2 [25]. This law can be written as

$$\ln P= \ln a + n \ln d \text{----(5.5)}$$

The plots of $\ln p$ versus $\ln d$ (d = indentation diagonal length, p = applied load), follow the Meyer's law [30 - 33], with different n values for different load ranges. These plots are shown in Figure 5.3 for $\text{InBi}_{1-x}\text{Te}_x$ ($x= 0, 0.05, 0.1$ and 0.15) crystals, respectively. Meyer's index is on the slope of the graph. Table-5.1 displays the Meyer index values derived in this instance. In the high load range, it is shown to be closer to $n=2$, indicating hardness saturation in this load range. It can be seen that in the low load range $n>2$. This implies that the surface penetration by the indenter causes severe deformation, work hardening takes place and as a result H_v reaches a high value becoming constant in the higher load range.

Table 5.1: Meyer index of $\text{InBi}_{1-x}\text{Te}_x$ crystals

Crystals	Lower load Meyer Index	Higher load Meyer Index
InBi	4.34	2.09
$\text{InBi}_{0.95}\text{Te}_{0.05}$	4.19	2.11
$\text{InBi}_{0.90}\text{Te}_{0.10}$	4.19	2.00
$\text{InBi}_{0.85}\text{Te}_{0.15}$	4.07	2.06

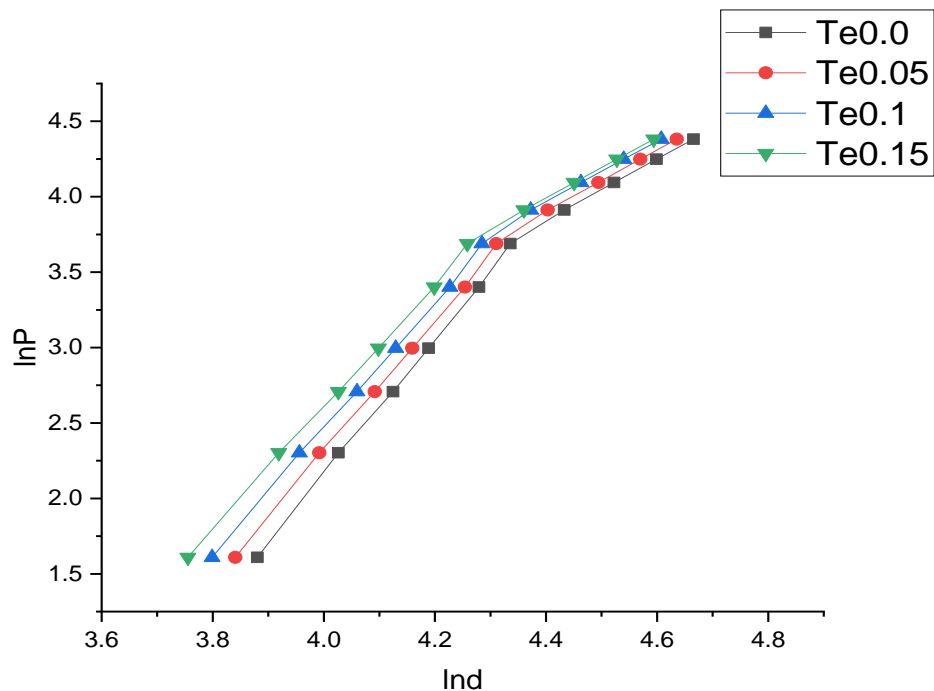


Figure 5.3: Plots of $\ln p$ vs $\ln d$ $\text{InBi}_{1-x}\text{Te}_x$ ($x= 0, 0.05, 0.1$, and 0.15) crystals

5.4 Effect of Annealing:

3mm thick freshly cleaved crystals were enclosed in an ampoule under vacuum at 10^{-4} torr. The sample temperature was kept at 80 °C for 24 hours, and then reduced to room temperature at a rate of 30°C per hour until it reached room temperature. Afterward, the microhardness measurements were performed with the pyramidal Vickers diamond indenter. Figures 5.4 (a-d) show load dependence of microhardness H_v on applied load P after the annealing process on $\text{InBi}_{1-x}\text{Te}_x$ ($x=0, 0.05, 0.1$ and 0.15) respectively. The true microhardness values of annealed crystals $\text{InBi}_{1-x}\text{Te}_x$ ($x=0, 0.05, 0.1$ and 0.15) obtained are 105, 111, 119, 125 MPa, respectively, which are quite less than that of the as-cleaved sample. Therefore, it may be concluded that annealing results in softening of the crystal. Annealing is expected to reduce the density of dislocations and loosen the immovable dislocation tangles. As a result, the crystals become softened; this phenomenon is mostly dependent on dislocation mobility.

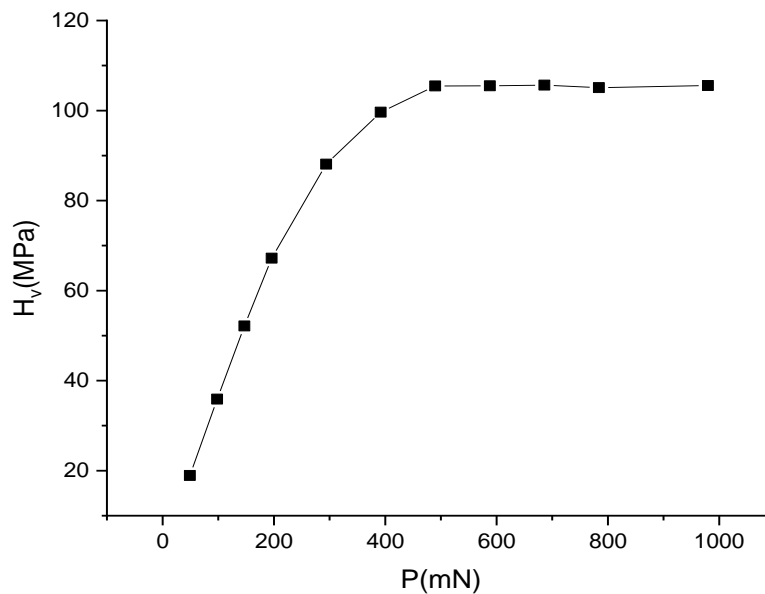


Figure 5.4(a): Plot of H_v versus P of InBi crystals annealed crystals

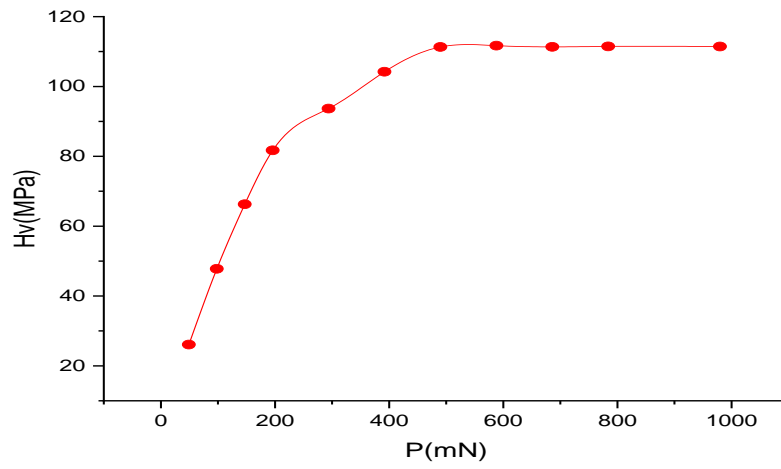


Figure 5.4(b): Plot of H_v versus P of $\text{InBi}_{0.95}\text{Te}_{0.05}$ crystals annealed crystals

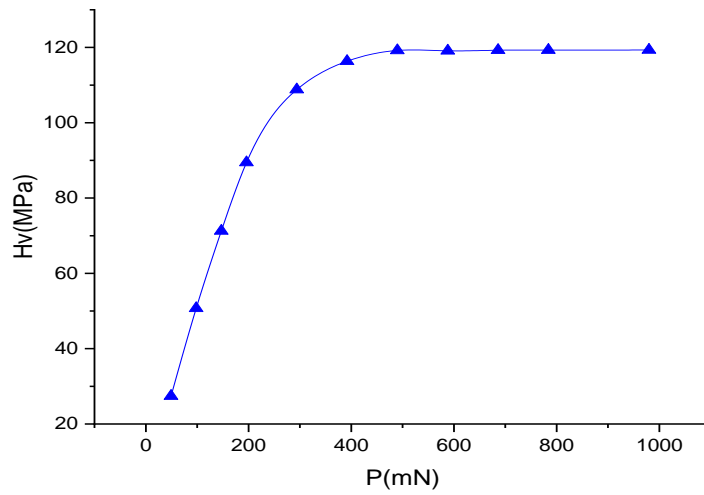


Figure 5.4(c): Plot of H_v versus P of $\text{InBi}_{0.9}\text{Te}_{0.1}$ crystals annealed crystals

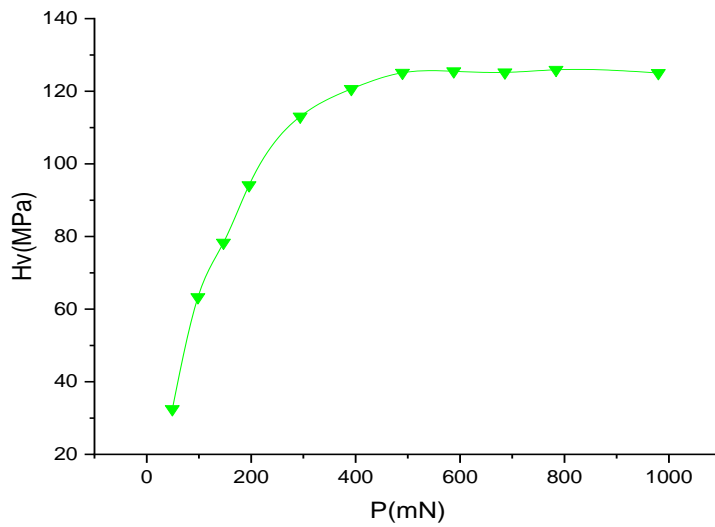


Figure 5.4(d): Plots of H_v versus P of $\text{InBi}_{0.85}\text{Te}_{0.15}$ crystals annealed crystals

5.5 Effect of Cold Working:

Cold work was carried out on the crystals prior to indentation to study the effects of work hardening on hardness. This was accomplished by placing two flat glass slabs, one on top of another and cleaved crystal in the form of 1 mm thick slice placed between them. A load of about 1.5 kg was placed on top of that. The compression was thus produced along the 'C' axis of the crystal and lasted for 24 hours at room temperature and then indentations were performed at varying loads using Vickers indenter. All crystals were treated with identical cold working. The cold work on the samples has resulted in a significant increase in load-independent microhardness. The dislocations will be more mobile in a softer crystal which will result in a greater tendency to strain harden. Figures 5.5 (a-d) show that the Vickers' microhardness H_v is load dependent up to some characteristic load in all the four cases with $x = 0, 0.05, 0.1, 0.15$ crystals, respectively, and also dependent on the condition whether the sample is as-cleaved, cold worked or annealed. The value in the saturation area is indicative of the bulk microhardness. Hence, it can be said that cold-work strain hardening is greater than as-cleaved strain hardening.

The following is an explanation of how cold-working affects low-load hardness. When the indenter penetrates deeper, rosette dislocations produce intersecting jogs and dipoles, which handle low-load deformation. As a result, a complex network of immobile dislocations will form in this region, functioning as a significant barrier to the movement of new dislocations.

The degree of interactions among the barriers and dislocations restricts the plastic flow at such depths, resulting in a hardness peak. The deformation-induced coherent area is a feature of mechanical condition of the crystal and it is the said depth zone wherein this occurs [13]. The above figures show that at low loads, hardness is load-dependent, whereas at greater loads, hardness is basically load-independent.

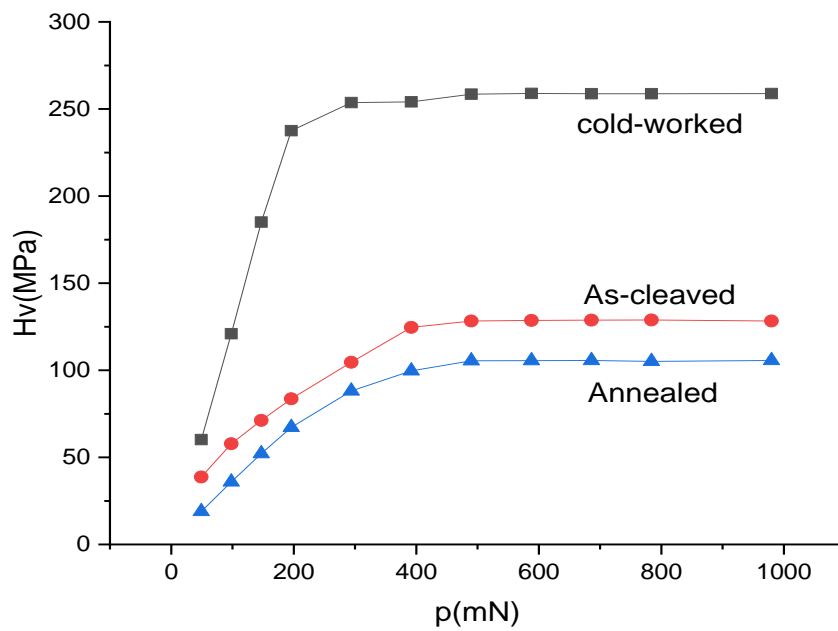


Figure 5.5(a): Plot of H_v versus P of InBi crystals

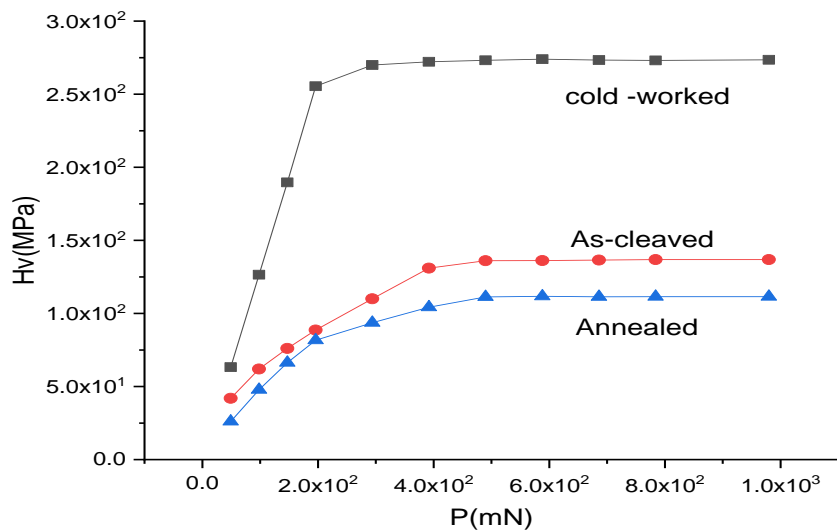


Figure 5.5(b): Plot of H_v versus P of InBi_{0.95}Te_{0.05} crystals

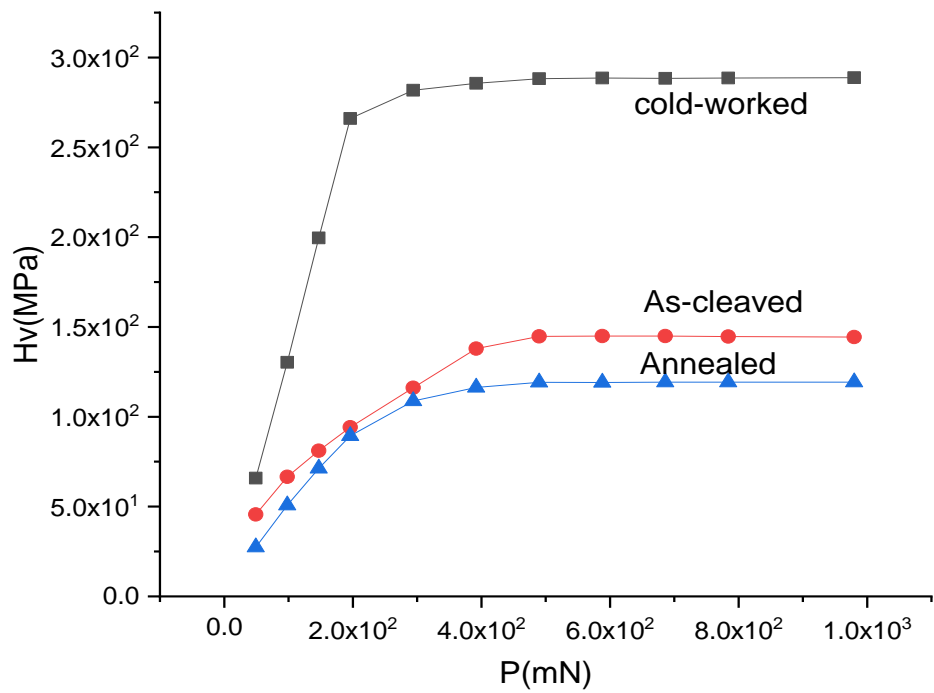


Figure 5.5(c): Plot of H_v versus P of $\text{InBi}_{0.9}\text{Te}_{0.1}$ crystals

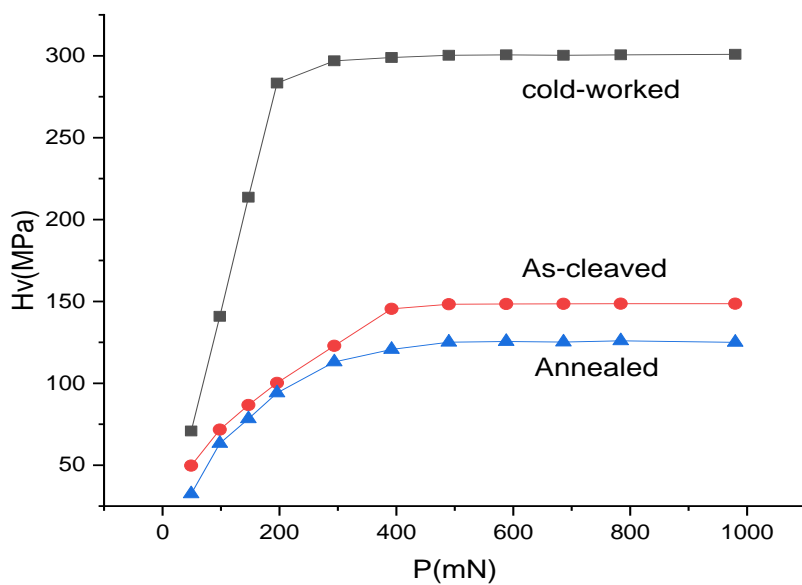


Figure 5.5(d): Plot of H_v versus P of $\text{InBi}_{0.85}\text{Te}_{0.15}$ crystals

5.6 Conclusions:

- Microhardness of $\text{InBi}_{1-x}\text{Te}_x$ ($x=0, 0.05, 0.1, 0.15$) crystals increases with concentration of Te.
- Microhardness of these crystals is dependent on load in the low load range.
- There is applied load dependence of hardness observed but the bulk micro hardness is found to be quite independent of the applied load.
- In the cold-worked crystals, the load independent hardness value significantly increases over that of the as-cleaved samples. In the annealed sample, the load independent hardness value is less than that of the as-cleaved sample.
- The annealing treatment very significantly improves perfection of all the crystals.

REFERENCES:

- [1] Shaw M. C., The Science of Hardness Testing and Its Research Applications, eds. J. H. Westbrook and H. Conrad (ASM, Ohio), (1973)
- [2] Tabor D., The Hardness of Metals (Oxford Univ.), (1951)
- [3] Bergsman E.B., Met. Progr., 54 (1948) 153
- [4] Rostoker W., J. Inst. Met., 77 (1950) 1975
- [5] Knoop F., Peters C. G. and Enerson, W. B., J. Res. Nat. Burstand, 23 (1939)
- [6] Bernhardt E. D., Metallk, 33 (1941) 135
- [7] Campbell R. F., Henderson O. and Dan leavy M. R., Trans. ASM, 40 (1948) 954
- [8] Taylor E.W., J. Inst. Met., 74 (1948) 493
- [9] Buckle H., Rev. Retall., 48 (1951) 957
- [10] Mott B.W., Ford. S. D. and Jones I. R. W., A.E.R.E. Harwell Report, 1R, 1 (1952) 017
- [11] Grodzinsky P., Indust. Diam. Rev., 12 (1952) 209, 236
- [12] Toman L. Jr., Nye W.F. and Gelas A.J., 5th Int. Cong. Electron microscopy, 1 (1962) FF – 13
- [13] Berzina I. G., Berman I. B. and Savintsev, P.A., Sov. Phys. Cryst., 9 (1965) 483
- [14] Gane N. and Cox J. M., Phill. Mag., 22 (1970) 881
- [15] Ivan'ko A. A., Handbook of Hardness Data, ed. G. V. Samsonov, (1971) 3
- [16] Hanemann H., Z. Metallk, 33 (1941) 124

- [17] Mil'vidskii M.G. and Liner L.V., Phys. Met. Metallog., 11 (1962) 96
- [18] Boyarskaya Y.S., Zavod. Lab., 4 (1960) 477
- [19] Yoshino T., Bull. J.S.M.E., 8 (1965) 291
- [20] Bhatt V. P, Desai C. F., Bull. Mater. Sci. 1982; 4: 23-28.
- [21] Walls M. G., Chaudhri M. M. and Tang T. B., J. Phys. D. Appl. Phys. (UK), 25, 3 (1992) 500 –7.
- [22] Onitsch E. M., Schweiz. Arch. Angew. Wiss., 19 (1953) 320.
- [23] Buckle H., Med. Rev., 4 (1959) 49.
- [24] Bochvar A. A. and Zhadaeva O. S., Bull. Acad. Sci. U.R.S.S.,3 (1947) 341.
- [25] Onitsch E.M., Mikroskopie, 2 (1947) 131.
- [26] Mott B. W., Micro-indentation hardness testing (Butterworths Scientific Publications, London), 1956; Ch 1.
- [27] Braunovic M., The Science of Hardness Testing and its Research Applications, Eds. J H. Westbrook and H. C. Conrad (ASN, Ohio), 1973,329.
- [28] Soni P. H., Physica B: Physics of Condensed Matter, 2018; 530: 157-15.
- [29] Hanemann, H. Z. Metallk, 33(1941) 124.
- [30] Buckle H, Progress in micro-indentation hardness testing, 2014; 50-51.
- [31] Meyer L, Micro-indentation hardness testing (Butterworths Scientific Publications, London), 1956; Ch 4.
- [32] C. F. Desai, P. H. Soni and S. R. Bhavsar, Ind. J. Pure and Appl. Phys., 37 (1999) 119-121.
- [33] C. F. Desai, Maunik Jani, P. H. Soni and G. R. Pandya, J. of Mater. Sci., 44 (2009) 3504-07.